Supporting Information: Quantitative Impact of Fluid vs. Solid Interfaces on the Catalytic Performance of Pickering Emulsions

Sebastian Stock,[†] Annika Schlander,[‡] Maresa Kempin,[¶] Ramsia Geisler,[†] Dmitrij Stehl,[†] Kai Spanheimer,[†] Nicole Hondow,[§] Stuart Micklethwaite,[§] Ariane Weber,[‖] Reinhard Schomäcker,[‖] Anja Drews,[¶] Markus Gallei,[⊥] and Regine von Klitzing*[,†]

†*Department of Condensed Matter Physics, Technische Universität Darmstadt, Darmstadt*

‡*Ernst Berl-Institute for Technical and Macromolecular Chemistry, Technische Universität Darmstadt, Darmstadt*

¶*Department II, Process Engineering in Life Science Engineering, HTW Berlin, Berlin*

§*School of Chemical and Process Engineering, University of Leeds, Leeds*

‖*Department of Technical Chemistry, Technische Universität Berlin, Berlin*

⊥*Polymer Chemistry, Saarland University, Saarbrücken*

E-mail: klitzing@smi.tu-darmstadt.de

Phone: +49-(0)6151-16-24506

S1 Theory

The comparison between the resulting internal emulsion interface after the emulsification process to the known total internal surface of the particles is a suitable approach to get further insights in emulsification efficiency and the surface conformation of the particles at the interface. The model describes the case when the initial coalescence occurring right

after the emulsification took place and internal surface is so far reduced that the number of particles is sufficient to stabilize the emulsion at this semi stable state for a long time. In preparation to apply the limited coalescence model in the present system it is possible to determine the specific internal particle surface from the Sauter mean diameter using simple geometric relations. For a spherical particle system consisting of different sized spheres the definition of the Sauter mean diameter d_{32} is:

$$d_{32} = \frac{1}{A_{\mathrm{p,tot}}} \sum_{i=1}^{N_p} d_{\mathrm{p},i} \pi d_{\mathrm{p},i}^2 = \frac{6 V_{\mathrm{p,tot}}}{A_{\mathrm{p,tot}}} \tag{1}$$

with N_p the total number of particles, $d_{\mathrm{p},i}$ the diameter of particle i, $A_{\mathrm{p,tot}}$ the total particle area and $V_{\mathrm{p,tot}}$ the total particle volume. In the next step the occupation of the total droplet area with particles is considered. It is assumed that the incident angle of the particles is $\theta = 90°$, i. e. each particle occupies a droplet area of $A_{\emptyset} = \frac{1}{4}\pi (d_{3,2})^2$. For a known average particle density ρ_{p} and the measured total mass of the used particles $m_{\mathrm{p,tot}}$ one receives for the total particle cross section $A_{\emptyset,\mathrm{tot}}$ per total mass of the particles $m_{\mathrm{p,tot}}$:

$$a_{\emptyset,\mathrm{m}} = \frac{A_{\emptyset,\mathrm{tot}}}{m_{\mathrm{p,tot}}} = \frac{3}{2\,\rho_{\mathrm{p}}\,d_{3,2}} \tag{2}$$

The relation for the total internal cross section for a spherical particle system depends on the average particle density and the particle Sauter mean diameter. These particle properties need to be determined experimentally. If the volume of the total system $V_{\mathrm{PE,tot}}$ is kept constant the following expression for the total emulsion interface $A_{\mathrm{w/o,tot}}$ in dependence from the PEs Sauter mean diameter d_{PE} and the water fraction f_w can be obtained using again the definition of the Sauter mean diameter:

$$A_{\mathrm{w/o,tot}} = \frac{6 V_{\mathrm{PE,tot}}}{d_{\mathrm{PE}}} f_w \tag{3}$$

Assuming that all particles adsorb at the interface the packing parameter s connects the total particle cross section with the internal interface of the emulsion:

$$A_{\emptyset,\mathrm{tot}} = sA_{\mathrm{w/o,tot}} \tag{4}$$

The densest physically possible packing for a system with equally sized spheres would be the close hexagonal packing with a packing parameter of $s = \frac{\pi}{2\sqrt{3}} \approx 0.907$. This leads to the following prediction for the droplet diameter in dependence of different measurable particle and emulsion properties:

$$d_{\mathrm{PE}} = \frac{6sV_{\mathrm{PE,tot}}}{a_{\emptyset,\mathrm{m}} m_{\mathrm{p,tot}}} f_w \tag{5}$$

With $c_{\mathrm{p}} = \frac{m_{\mathrm{p,tot}}}{m_{\mathrm{PE,tot}}}$ as particle concentration eq. (5) can be transferred to:

$$d_{\mathrm{PE}} = \frac{6sf_w V_{\mathrm{PE,tot}}}{a_{\emptyset,\mathrm{m}} m_{\mathrm{PE,tot}}} \frac{1}{c_{\mathrm{p}}} \tag{6}$$

with $m_{\mathrm{PE,tot}}$ as the total emulsion mass.

One can show that the total void area $A_{\mathrm{void,tot}}$ is not directly dependent on the particle size:

$$A_{\mathrm{void,tot}} = A_{\mathrm{w/o,tot}} (1 - s) = A_{\emptyset,\mathrm{tot}} \frac{1 - s}{s} \tag{7}$$

But the size of one gap is in fact dependent from the particle size:

$$A_{\text{single void}} = \left(\sqrt{3} - \frac{1}{2}\pi\right) r_{3,2}^2 \approx 0.16\, r_{3,2}^2 \tag{8}$$

The size of one void scales square with the input particle diameter. It shows that using 100 nm spheres instead of 50 nm spheres of equal total surface the single voids in the 100nm system are fewer but 4 times larger. Therefore the mass transport should be easier in the

100nm particle system and if the reaction system was limited by the mass transport using larger spheres should be beneficial for the yield under the assumption similar total particle area were used.

The total substrate contact area $A_{\text{oil contact}}$ (oil-Si + oil-water) can be calculated using the total particle surface $A_{\text{PE,tot}}$ to:

$$A_{\text{oil contact}} = A_{\text{void,tot}} + \frac{1}{2}A_{\text{PE,tot}} = A_{\emptyset,\text{tot}}\left(\frac{1-s}{s} + 2\right) = A_{\emptyset,\text{tot}}\frac{1+s}{s} \tag{9}$$

assuming that in average one half of the spheres extends into the oil phase (three phase contact angle 90°). This is again not dependent from the particle size.

S1 Particle characterization

Transmission Electron Microscopy (TEM) TEM was used to determine the particle size and shape. A drop (8 μl) from a particle suspension in ethanol was put on a Cu TEM grid with carbon film using a microliter pipette. The particle concentration was 0.027 wt% for the smaller particles and 0.1 wt% for the larger particles. The ethanol was allowed to evaporate from the TEM grid until it was completely dry. The samples were then examined with the FEI CM 20 ST transmission electron microscope

Spin Coating Before use the silicon wafers were etched in piranha solution H_2O_2:H_2SO_4 (3:1) for 30 min. For the negatively charged particles the wafer were coated with 0.01 wt% solution of PEI first. The particle suspension containing 1 wt% particles was then put on a wafer (300 μl on 25 mm $\times$ 25 mm) until the wafer was covered with liquid. After a waiting time of 2 min the wafer was rotated with 1000 rpm for 2 more minutes using the spincoater Model WS-400B-6NPP-LITE by Lawel Technology Cooperation.

Atomic Force Microscopy (AFM) The obtained particle layer on top of the wafers were examined in detail with a JPK nanowizard atomic force microscope. An AC160TS cantilever was used in intermittent contact mode to scan the surface. The surface roughness was determined on at least three different places with a size of $2\,\mu\mathrm{m} \times 2\,\mu\mathrm{m}$ and the average was taken as a value and the standard deviation as a hint for the measurement error.

Sessile Drop Sessile drop measurements were carried out with a dataphysics OCA 15 dropshape analyzer (DSA) with a drop volume of $3.5\,\mu\mathrm{l}$ using the Young-Laplace fitting method. The contact angle was measured for 1 min carrying out a measurement every second. From an average of at least five different drops the average value and standard deviation as an indicator for the error was calculated.

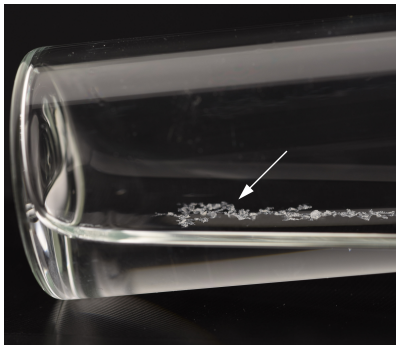

Figure S1: The hydrophobized 50C18n+ particles float on the water surface. This simple test is a strong hint for the success of the surface modification.

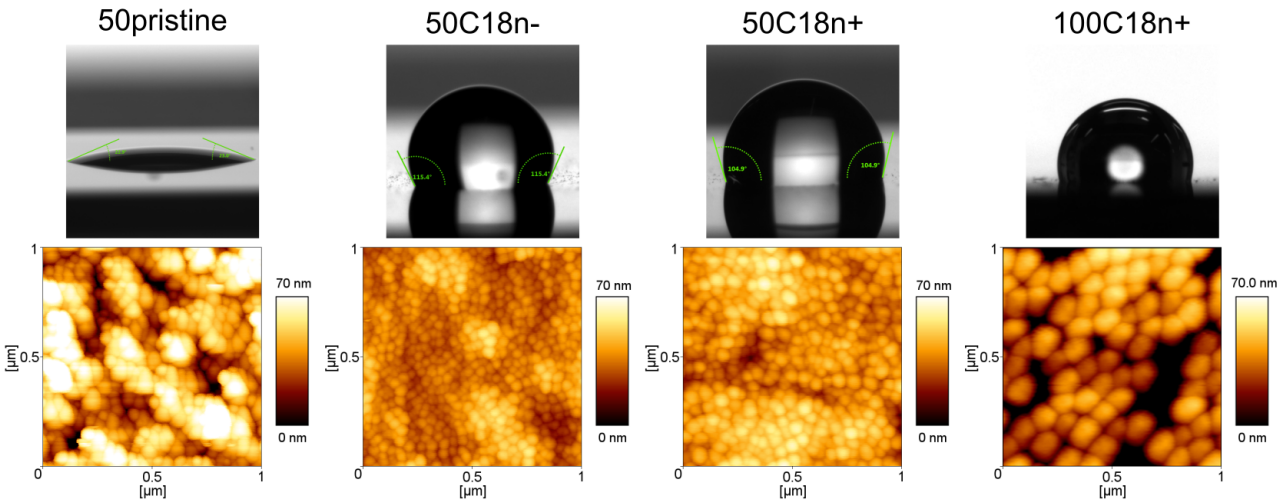

	50pristine	50C18n-	50C18n+	100C18n+
Contact angle / °	24 ± 4	113 ± 3	107 ± 4	105 ± 3
RMS Roughness / nm	18 ± 3	13 ± 4	17 ± 4	29 ± 8

Figure S2: Top row: 3.5 μl water droplets on top of a wafer spin coated with modified particles. Second row: AFM images of the particle layers used for the contact angle determination. Bottom row: Measured contact angles of a water droplet on top of the particle layer with the corresponding measured layer roughness.

ζ-Potential Measurement The ζ-potential of the particles was determined at particle concentrations of 0.02 wt% using a Malvern Zetasizer Nano in ethanol. The sample cell was purged with ethanol and water and was tested before and after the measurements with a standard. Different vials with ethanol containing equal particle concentration were prepared and different catalyst concentrations were added to each vial. After 10 minutes in the ultrasonic bath the ζ-potentials of the particles in the mixtures containing now different amounts of SX were measured.

Particle density measurements The particle density was determined indirectly measuring the total density solutions with a known particle concentration and calculating the

particle density from the resulting slope value. The density of the dispersions were measured with the densiometer DM40 from Mettler Toledo which based on a flexural resonator. The precision is given as 0.001 $\frac{\mathrm{g}}{\mathrm{cm}^3}$. The instruments reliability was checked after every measurement with a pure water sample. For the total suspension density ρ_{tot} as a function of particle concentration with the assumptions that the total mass m_{tot} of the dispersion is the addition of the mass of the liquid m_{l} and the mass of the solid part $m_{\mathrm{p,tot}}$ one receives the following expression:

$$\frac{1}{\rho_{\mathrm{tot}}} = \frac{1}{\rho_{\mathrm{l}}} + \frac{\rho_{\mathrm{p}} - \rho_{\mathrm{l}}}{\rho_{\mathrm{p}} \cdot \rho_{\mathrm{l}}} x_{\mathrm{p}} \tag{10}$$

With the particle concentration x_{p} defined as $x_{\mathrm{p}} = \frac{m_{\mathrm{p,tot}}}{m_{\mathrm{tot}}}$ and the densities ρ_{p} and ρ_{l} for the density of the particles and the density of the liquid respectively. The expression shows that the particle density can be determined from the slope in the reciprocal plotted total density over the particle concentration.

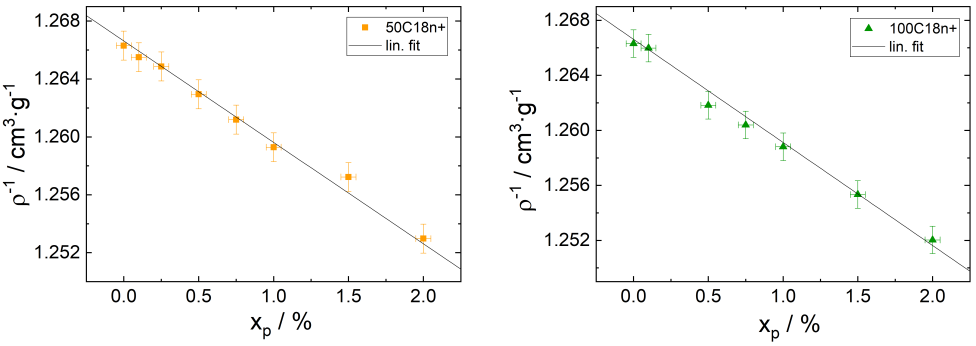

a) 50C18n+ **b)** 100C18n+

Figure S3: The average particle density was deducted from the reciprocal density of suspensions with increasing particle concentration. The slope is proportional to the particle density. The reciprocal solvent density was determined and fixed in the linear approximation. Density values of $(1.77 \pm 0.04)\ \frac{\mathrm{g}}{\mathrm{cm}^3}$ for the smaller and $(1.93 \pm 0.05)\ \frac{\mathrm{g}}{\mathrm{cm}^3}$ for the larger particles were determined.

S4-S8 Microscopy of PEs

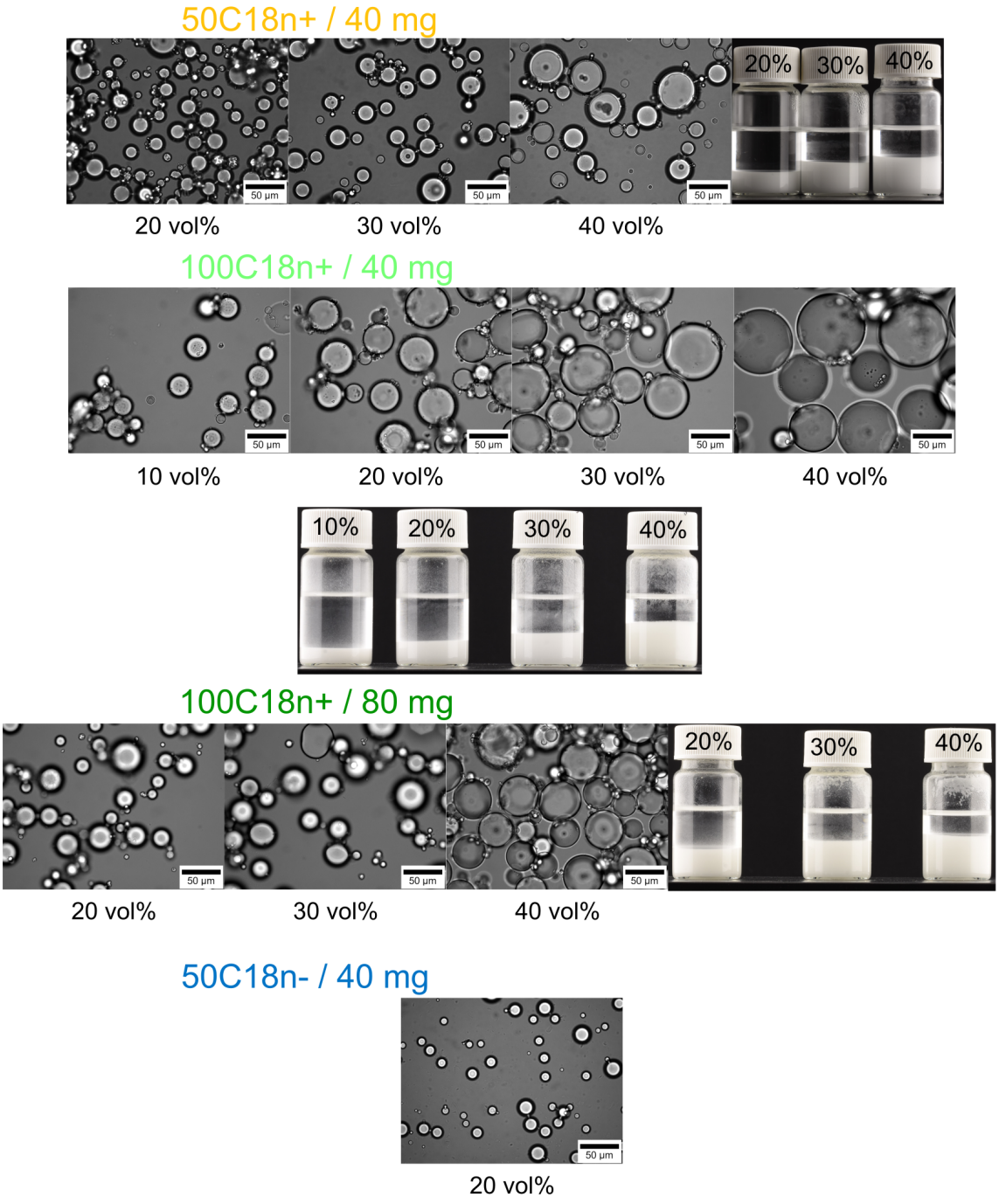

Figure S4: Selection of microscopy images of the prepared PEs with different particles and different water fractions with the corresponding photographs of the PEs. At least 15 of these images of each sample containing in total 400 to 800 droplets were used for the determination of the Sauter mean droplet diameter in dependence of the water fraction. The Photographs show the sedimentation of the PEs after a few hours. The droplets themself stay intact.

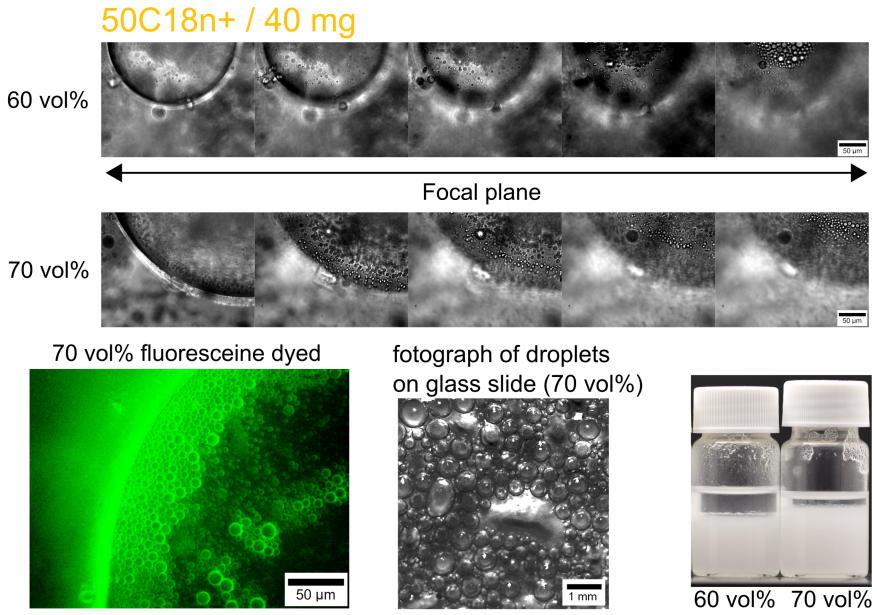

Figure S5: The structure of PEs with a water fraction above 50 vol% deviate fundamentally from PEs with water fractions below 50 vol%. Top: Micrographs of PEs prepared with water fractions of 60 vol% and 70 vol%. Very large and very small droplets are observed. When moving the focal plane of the microscope towards the bottom of the larger droplet the smaller droplets become visible. The small droplets occur only inside the large droplets but not in the continuous phase outside the droplet. Bottom: The fluorescein dyed version of the 70 vol% PE indicates that the smaller droplets are water droplets in agreement with the small droplets in the large droplets. A photograh of the droplets spred on a glass slide shows the scale of the larger droplets. The photographs on the right show the macroscopic PEs.

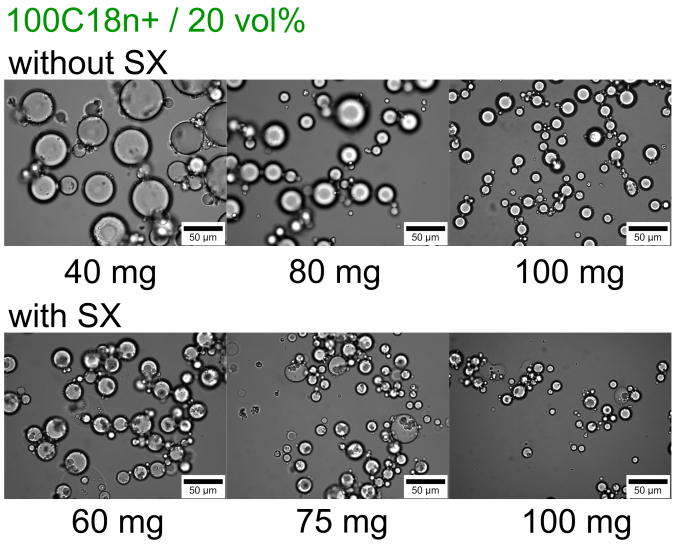

Figure S6: Micrographs of PEs prepared with and without the ligand SX in dependence of the particle concentration. PE total volume 12.55 ml, 20 vol % water fraction and 0.015 $\frac{\text{mol}}{\text{l}} \approx 147$ mg SX.

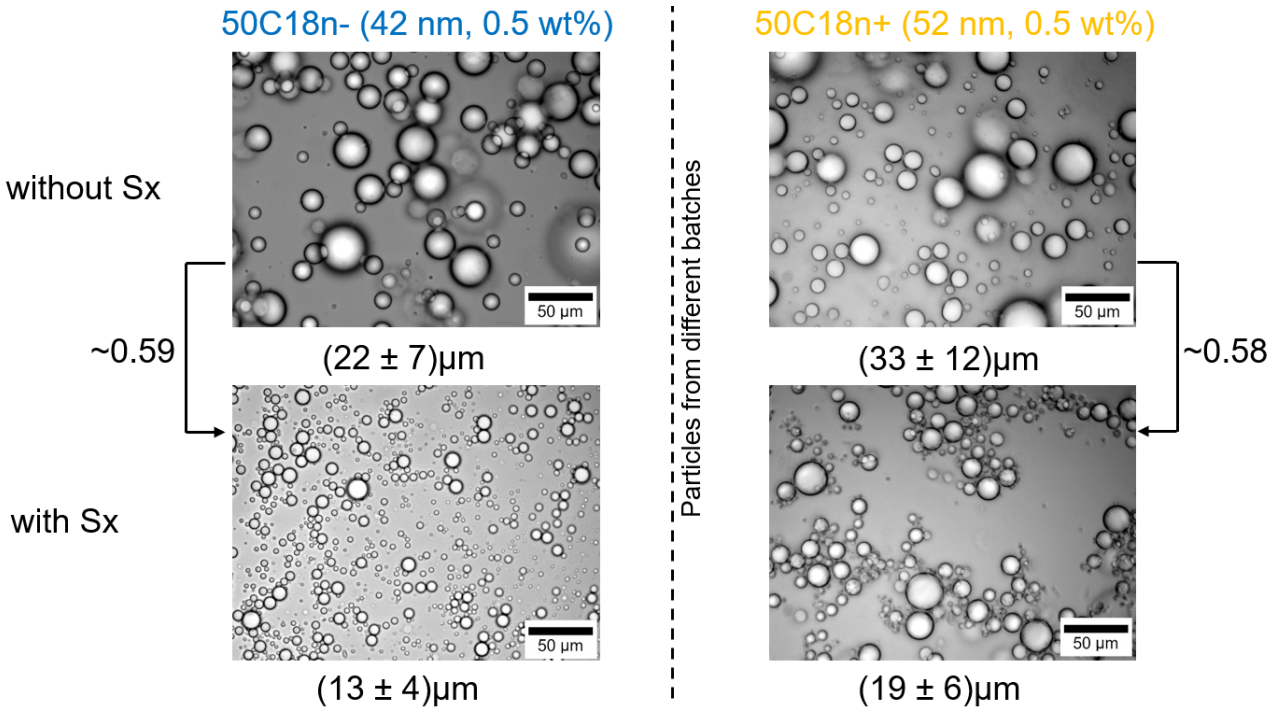

Figure S7: Micrographs and droplet size measurements with a slightly smaller sized particle batch of 50C18n- particles ($d_{3,2} = 41.5\,\mathrm{nm}$) and a slightly larger batch of 50C18n+ modified particles ($d_{3,2} = 52.6\,\mathrm{nm}$) than the particles studied above with a concentration of 0.5 wt% and a water fraction of $f_\mathrm{w} = 20\,\mathrm{vol}\%$ show also the effect of an decrease in packing parameter. The Sauter mean droplet diameter for the negatively charged 50C18n- particles decreased with the addition of SX from $d_{3,2} = 22\,\mu\mathrm{m}$ to $d_{3,2} = 13\,\mu\mathrm{m}$ and for the positively charged 50C18n+ particles from $d_{3,2} = 33\,\mu\mathrm{m}$ to $d_{3,2} = 19\,\mu\mathrm{m}$. This represents a decrease in both cases of roughly 40 % $c_\mathrm{SX} = 0.015\,\frac{\mathrm{mol}}{\mathrm{l}}$.

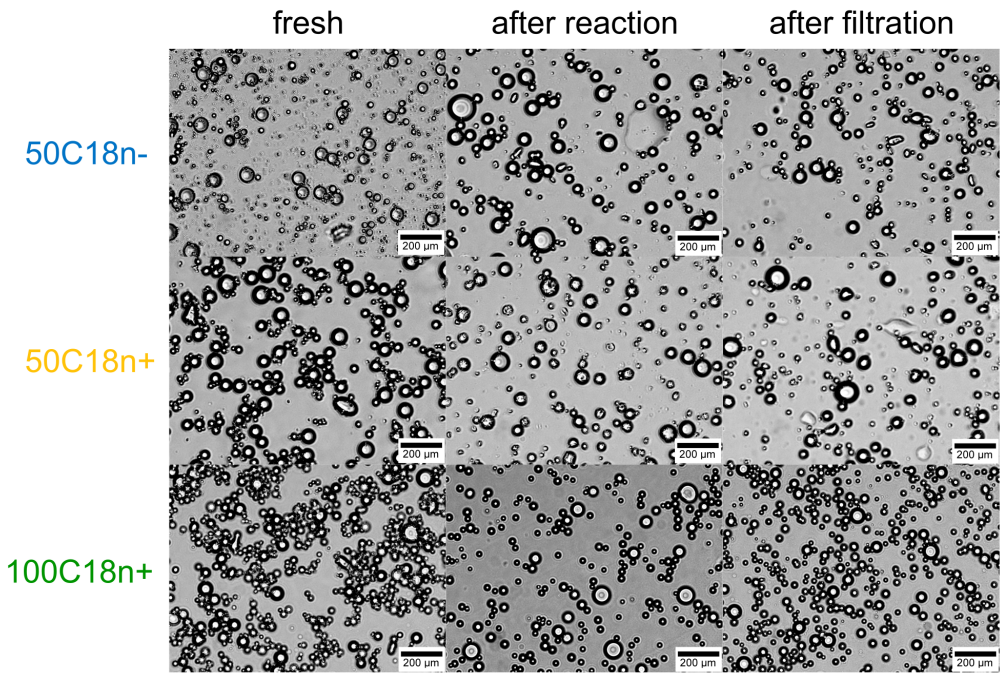

Figure S8: Micrographs of PEs used for the reaction. The droplet sizes were determined before and after the reaction as well as after the filtration. For the droplet size determination more than 15 images were used.